High-Speed Fiber-Optic Communication Performance Utilizing Fiber Bragg Grating-Based Dispersion Compensation Schemes

Kripa Kalkala Balakrishna[1], Karthik Palani[2]*
Research Scholar, Cambridge Institute of Technology, K.R. Puram, Bengaluru-560036, Karnataka, India[1]
Affiliated to Visvesvaraya Technological University, Belagavi – 590018, Karnataka, India[1]
Professor, Department of Information Science Engineering, Cambridge Institute of Technology, K.R. Puram, Bengaluru- 560036, Karnataka, India[2]

Abstract*—Chromatic dispersion is a significant limitation in optical fiber communication, as it causes pulse broadening, which negatively impacts transmission distance and data rates, both of which are critical for meeting the high-speed demands of 5G optical networks. This study focuses on addressing chromatic dispersion in Standard Single-Mode Fiber (SSMF) systems, which are widely deployed in 5G fronthaul and access networks. A comprehensive investigation is conducted using Gaussian-apodized linear chirped Fiber Bragg Gratings (FBGs) for dispersion compensation, implemented across three strategic configurations: pre-compensation, post-compensation, and symmetrical compensation. Each scheme is systematically evaluated to determine the most effective approach for enhancing signal integrity and overall network performance. Simulations are performed using OptiSystem 7.0 on a 10 Gbps SSMF-based optical system, with transmission distances ranging from 10 km to 80 km under controlled simulation parameters. Key performance metrics, including Quality factor (Q-factor), Bit Error Rate (BER), and eye height, are analyzed by varying SSMF length, input power, and bit rate. The results demonstrate that symmetrical compensation using Gaussian-apodized linear chirped FBGs provides the best performance, achieving a Q-factor of 12.3938, an ultra-low BER of 1.12336×10^{-35}, and a significantly improved eye height at 80 km. These findings establish the symmetrical compensation scheme employing Apodized Chirped Fiber Bragg Gratings (ACFBGs) as the most effective and scalable solution for high-speed, long-distance optical transmission in 5G networks. This approach enables key 5G applications, including ultra-reliable low-latency communication (URLLC), enhanced mobile broadband (eMBB), and smart infrastructure in smart cities. The proposed technique offers multiple advantages, such as low BER, high Q-factor, reduced signal distortion through sidelobe suppression, energy efficiency via passive operation, and design flexibility for long-haul network integration.

Keywords*—Dispersion management; chirped fiber bragg grating; gaussian apodization; quality factor; bit error rate; optical transmission system

I. Introduction

High-speed optical communication systems rely on laser sources that emit nearly monochromatic light with a narrow spectral linewidth. As optical signals propagate through SSMFs, different wavelength components propagate at different velocities, leading to temporal spreading of the optical signal. This phenomenon leads to pulse overlap, commonly known as Intersymbol Interference (ISI), which is primarily caused by chromatic dispersion. In SSMFs, chromatic dispersion typically ranges from 15 to 20 ps/nm/km, and its impact becomes increasingly severe with longer transmission distances and higher bit rates. Chromatic dispersion in optical fibers arises from two main components: material dispersion (MD) and waveguide dispersion (WD). In single-mode fibers, material dispersion is generally the predominant factor, arising from the refractive index of the fiber material varying with wavelength [1]. In long-haul, high-speed optical networks, the primary impairments to signal quality include attenuation, nonlinear effects, and chromatic dispersion. While attenuation can be mitigated using Erbium-Doped Fiber Amplifiers (EDFAs) and nonlinearities managed by optimizing input power levels, chromatic dispersion remains the most critical limiting factor. Due to its minimal attenuation, the 1550 nm window is commonly used in optical communication systems [2].

To address chromatic dispersion in optical fiber systems, several compensation methods have been developed, such as Dispersion-Compensating Fibers (DCFs), Dispersion-Shifted Fibers, and Fiber Bragg Gratings (FBGs). Among these, DCFs offer negative dispersion to counterbalance the positive dispersion of SSMFs, but they can increase system cost and introduce nonlinear effects. Therefore, FBGs are preferred as a more compact, passive, and low-loss alternative [3–5].

FBGs are typically categorized into Uniform Fiber Bragg Gratings (UFBGs), which have constant grating periods, and Chirped Fiber Bragg Gratings (CFBGs), whose grating periods vary along their length. CFBGs can incorporate different apodization profiles and chirp functions, allowing the grating period to vary in a linear, quadratic, or cubic manner. Among these, Linear CFBGs are widely regarded as an effective solution for chromatic dispersion correction and compensation due to their ability to reflect different wavelengths at different spatial locations, thereby introducing wavelength-dependent delays and mitigating pulse broadening [6]. In addition, they are immune to nonlinear effects and are well-suited for high-speed optical systems. To further enhance performance, apodization techniques are employed. Apodization involves a gradual modulation of the refractive index profile, which suppresses

*Corresponding Author

side lobes in the reflection spectrum and reduces signal distortion. This leads to the development of ACFBGs, which provide superior dispersion compensation with improved signal quality [7–9].

EDFAs are commonly used to amplify optical signals in long-distance systems, while dispersion compensation can also be assisted by optical filters, such as Gaussian, Bessel, and Fabry-Pérot filters, at the receiver end [10]. As bit rates approach 40 Gbps, chromatic dispersion becomes a critical factor limiting system performance [11]. Although single-mode fibers are capable of supporting high-speed data rates, they still suffer from signal degradation due to attenuation and dispersion-induced waveform distortion, which contributes to ISI and crosstalk [12–14]. The Q-factor and BER are key parameters that determine the achievable transmission distance in optical communication systems. For reliable performance, the system should maintain a Q-factor above 6 and a BER below 10^{-9} to ensure signal integrity over long distances [15–17].

Despite extensive research into dispersion compensation using CFBGs and DCFs, most existing studies focus on a single compensation scheme, typically either pre- or post-compensation schemes under fixed system configurations. Systematic comparisons of all three strategies (pre-, post-, and symmetrical), particularly using Gaussian-apodized CFBGs, are rarely explored. Additionally, few works have evaluated performance at extended distances (e.g., 80 km) or considered the combined impact of key parameters such as transmission length, bit rate, and input power. This lack of holistic analysis presents a gap in identifying the most effective dispersion compensation approach designed for long-distance, high-speed optical communication systems.

To bridge this gap, the present study designs and evaluates Gaussian-apodized linear CFBGs across three compensation schemes: pre-, post-, and symmetrical. Simulations are conducted in OptiSystem 7.0 over transmission distances spanning 10 km to 80 km, input power levels from 1 dBm to 10 dBm, and data rates varying between 5 Gbps and 20 Gbps. The results indicate symmetrical compensation consistently delivers superior dispersion mitigation, particularly at extended distances and lower power levels.

A. Key Contributions of this Study Include

- Design and optimization of ACFBG models with Gaussian apodization and linear chirp profiles to enhance dispersion compensation.
- Evaluation of pre-, post-, and symmetrical compensation methods, highlighting their respective advantages and limitations.
- Assessment of signal quality and transmission integrity using key evaluation metrics, including BER, Q-factor, and eye height, under different compensation scenarios.
- Validation of the proposed ACFBG designs and compensation schemes via simulation, demonstrating their feasibility for practical applications in long-haul and metropolitan networks.

The structure of this study is organized as follows: Section II reviews the related work; Section III introduces the fundamental concepts; Section IV describes the methodology; Section V presents the simulation results; Section VI provides a discussion of the findings; Section VII concludes the study and outlines potential directions for future work.

II. Related Works

Numerous studies have investigated dispersion compensation techniques in optical fiber systems, with a particular focus on the use of FBGs and DCFs in various configurations.

Murooj A. Abd Almuhsan [18] implemented a post-compensation system using both DCF and FBG over a 50 km SSMF link at 10 Gbps in OptiSystem 12.0. By using an FBG having a dispersion coefficient of −2000 ps/nm, the system achieved outstanding performance with a Q-factor of 45.78, BER of 0, and eye height of 6.9×10^{-14}.

Keti [19] proposed a post-compensation model using a linear CFBG featuring tanh apodization and a Gaussian low-pass filter. Over a 40 km fiber span. The resulting Q-factor and BER of the system were 29.55 and 9.34×10^{-18}, outperforming both uniform FBG and uncompensated setups. This study emphasizes the impact of apodization and filtering in enhancing dispersion compensation.

Mustafa et al. [20] showed that the post-compensation scheme with raised sine apodization delivered the best results in a four-cascaded apodized linear CFBG model using the Multichannel Time Division Multiplexing (MTDM) approach. In a 10 Gbps WDM transmission over 70 km utilizing 2 mm-long gratings, the system attained a Q-factor of 8.58 with a BER of 4.77×10^{-18}. By comparison, the pre-compensation approach using a raised cosine apodization achieved a Q-factor of 7.664 and BER of 8.99×10^{-15}, while the symmetrical compensation scheme with a raised sine profile resulted in a Q-factor of 7.49 and BER of 3.53×10^{-14}.

Mustafa et al. [21] reported that the post-compensation approach delivered the superior performance in their introduction of a UFBG model employing single-stage tanh apodization within the MTDM framework for a 10 Gbps WDM system spanning a 70 km optical link, this configuration achieved a Q-factor of 9.2 along with an exceptionally low BER of 3.25×10^{-20}. In comparison, the pre-compensation approach achieved a Q-factor of 9.13 and a BER of 3.4×10^{-20}, whereas the symmetrical compensation method resulted in a Q-factor of 8.8 and a BER of 8.22×10^{-19}.

Panda et al. [22] employed an FBG-based post-compensation design for an 80 km fiber link, resulting in a Q-factor of 6.85 and a BER of 3.73×10^{-12} using 2 mm and 3 mm gratings, showcasing the practicality of FBGs in long-distance links.

Chakkour et al. [23] designed a post-compensation scheme combining UFBGs with an EDFA in a 10 Gbps WDM system. Over a 10–30 km span, the system achieved Q-factors up to 81.47 and showed strong optical gain, demonstrating potential in short-distance high-speed links.

Mustafa et al. [24] proposed a post-compensation scheme using a four-cascaded CFBG model with Differential Phase-Shift Keying (DPSK) modulation within a 10 Gbps WDM system deployed across a 70 km fiber link. The system utilized 5 mm FBG gratings and achieved a Q-factor of 7.22 and a BER of 2.59×10^{-13}, demonstrating the effectiveness of cascaded CFBG for dispersion mitigation.

While previous studies have explored the use of CFBGs for dispersion compensation, most have focused on a single compensation scheme or operated under fixed system parameters, with limited use of Gaussian apodization and few comparative analyses. This study addresses these gaps by systematically evaluating pre-, post-, and symmetrical compensation using Gaussian-apodized linear CFBGs over varying SSMF lengths (10 to 80 km), input powers, and bit rates in OptiSystem 7.0. The results show that at 80 km, the symmetrical scheme outperforms previous FBG-based methods, highlighting its effectiveness for long-haul optical links.

III. Concepts and Principles

A. Principle of Fiber Bragg Grating

Ken Hill pioneered the first demonstration of an FBG in 1978. A FBG is created by inscribing periodic variations in the refractive index along the core of an optical fiber through exposure to a high-intensity optical interference pattern. This periodic modulation forms a grating that reflects a specific wavelength, known as the Bragg wavelength, while permitting other wavelengths to propagate through the fiber with minimal loss. As illustrated in Fig. 1, a UFBG maintains a constant grating period and index modulation, which allows it to reflect only the wavelength satisfying the Bragg condition. This makes it particularly advantageous for narrowband filtering in optical communication systems [25].

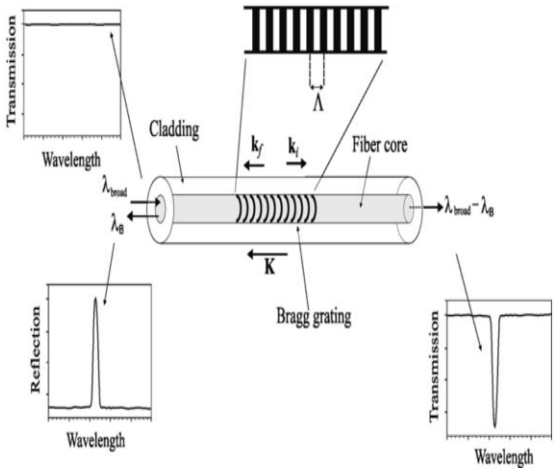

Fig. 1. UFBG with constant modulation amplitude and period.

The Bragg wavelength (λ_{Bragg}) is the specific wavelength reflected by the grating, is defined by Eq. (1):

$$\lambda_{Bragg} = 2n_{eff}\Lambda \quad (1)$$

Here, n_{eff} is used to indicate the effective index of refraction in the fiber core, and Λ denotes the periodic spacing of the grating [26]. This equation highlights that the reflected wavelength can be tuned by modifying either the refractive index or the grating period, enabling FBGs to support a wide range of optical applications.

B. Apodized Chirped Fiber Bragg Gratings (ACFBG) Structure and Mathematical Framework

CFBGs are used to compensate for chromatic dispersion in optical fibers by gradually varying the grating spacing distributed along the fiber length. This variation causes different wavelengths of light to reflect at different positions within the grating [27]. As a result, each wavelength experiences a different delay, enabling the recompression of optical pulses that have been broadened by dispersion.

In this process, shorter (faster) wavelengths reflect from regions with a smaller grating period, which are located deeper within the grating, resulting in longer delays. Conversely, longer (slower) wavelengths reflect from regions with a larger grating period, located closer to the input, and thus experience shorter delays. Because of their broad reflection bandwidth and non-uniform grating structure, CFBGs are widely employed to compensate for dispersion in high-speed optical systems [28], as shown in Fig. 2. Furthermore, the use of ACFBGs significantly enhances system performance by reducing side lobes and minimizing group delay ripple**,** making them particularly suitable for precise chromatic dispersion management in modern optical networks [29].

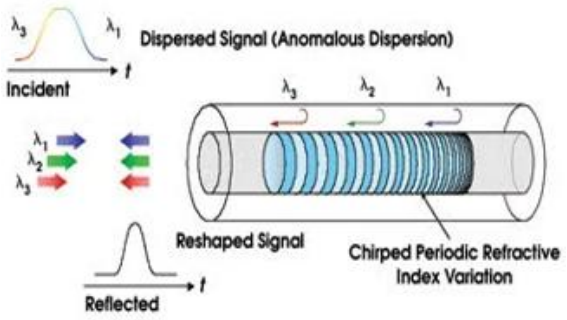

Fig. 2. Structure and operating principle of a CFBG.

The range of reflected wavelengths is expressed as Eq. (2):

$$\Delta\lambda_{chirp} = 2n_{eff}(\Lambda_L - \Lambda_S) = 2n_{eff}\,\Delta\Lambda_{chirp} \quad (2)$$

Here, $\Delta\lambda$chirp represents the difference from shortest to longest reflected wavelengths, denoted by λL and λS, respectively, while $\Delta\Lambda$chirp represents the variation between the longest ΛL and shortest ΛS grating period [30].

In a linear CFBG, the grating period at position z is defined as Eq. (3):

$$\Lambda_{(z)} = \Lambda_0 - \left[\frac{\left(\frac{z - Lg}{2}\right)}{Lg}\right]\Delta \quad (3)$$

where, Λ_0 is the midpoint period, *Lg* denotes the total grating length, while Δ represents the overall chirp [30]. Each wavelength reflects from a specific grating section, introducing a unique time delay.

The time delay τ (λ) experienced by a wavelength λ is given by:

$$\tau(\lambda) = \frac{\lambda - \lambda s}{\lambda L - \lambda s} \frac{2neffLg}{c} \quad (\lambda s \leq \lambda \leq \lambda L) \qquad (4)$$

Here, c signifies the speed at which light travels in a vacuum [30].

To determine the CFBG's dispersion in ps/nm/km, Eq. (4) is differentiated with respect to the wavelength λ, as in Eq. (5):

$$D(\lambda) = \frac{d\tau(\lambda)}{d\lambda} = \frac{1}{\lambda L - \lambda s} \frac{2neffLg}{c} \quad (\lambda s \leq \lambda \leq \lambda L) \qquad (5)$$

The refractive index profile $n(z)$ of an apodized linear CFBG is given by Eq. (6):

$$n(z) = n_0 + \Delta n_{dc}(z) + f_{A(z)} \Delta n_{ac}(z) \cos\left[\frac{2\pi}{\Lambda} z + \phi(z)\right] \qquad (6)$$

Here, n0 refers to the initial refractive index, fA(z) represents the apodization function, Δnac defines the modulation amplitude, Δndc is the average index change, and ϕ(z) is the phase [30]–[32].

The effective refractive index is therefore approximated as Eq. (7):

$$n_{eff} = n_0 + \Delta n_{dc} \qquad (7)$$

A Gaussian apodization function can be used to taper the refractive index modulation smoothly and is described as Eq. (8):

$$A_{(z)} = \exp\left\{-\ln 2 \left[\frac{2.(z - L/2)^2}{s.L}\right]\right\} \qquad (8)$$

Here, L represents the grating length, and s denotes the apodization strength parameter, and $z \in [0, L]$ [33].

IV. Methodology of the Proposed Framework

The proposed system setup, illustrated in Fig. 3, demonstrates a dispersion compensation design using an ACFBG. The input to the system is a binary data stream generated by a 10 Gbps Pseudo-Random Bit Sequence (PRBS) generator, which is then converted into Return-to-Zero (RZ) optical pulses. These pulses are modulated using a Mach–Zehnder Modulator (MZM) with an extinction ratio of 30 dB. The MZM encodes the data onto a continuous wave (CW) optical carrier with 3 dBm power, generated by a semiconductor laser operating at 193.4 THz. The modulated optical signal is transmitted through SSMF toward the receiver.

Dispersion compensation is performed at the receiver using an ACFBG featuring linear chirp and Gaussian apodization to improve performance by minimizing side lobes and group delay ripple. The system operates at a wavelength of 1550 nm. An EDFA optical amplifier with a 10 dB gain is used to enhance the signal strength before the detection. A PIN photodetector is employed for optical-to-electrical conversion, and the signal is further processed using a Low-Pass Gaussian Filter (LPGF) with a cutoff frequency set to 0.75 times the bit rate to suppress high-frequency noise.

System performance is evaluated using Q-factor, BER, and eye height, as observed through eye diagram analysis, with Q-factor serving as a key indicator of BER. All simulations are carried out in OptiSystem 7.0 by varying SSMF length, input power, and bit rate the relative performance of pre-, post-, and symmetrical compensation techniques is examined.

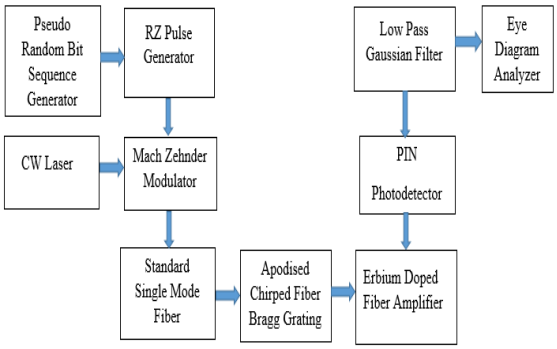

Fig. 3. Structural overview of the proposed design.

OptiSystem 7.0 was chosen for this study due to its advanced capabilities in modeling and simulating real-world optical communication systems. It effectively incorporates key transmission impairments, including chromatic dispersion, amplified spontaneous emission (ASE) noise, and nonlinear effects such as self-phase modulation. Its modular design enables flexible construction of complex system architectures, ranging from point-to-point links to WDM and long-haul transmission setups, by integrating standardized optical components such as fiber models, optical amplifiers, filters, and Fiber Bragg Gratings (FBGs).

In addition, OptiSystem offers a comprehensive suite of built-in analysis tools, including Q-factor measurement, BER estimation, and eye diagram visualization, which support both qualitative and quantitative performance evaluation. These features allow for controlled, repeatable testing across a wide range of parameters, making the platform highly suitable for validating dispersion compensation techniques in long-distance SSMF systems.

The overall simulation workflow is illustrated in Fig. 4, and the key simulation parameters are summarized in Table I.

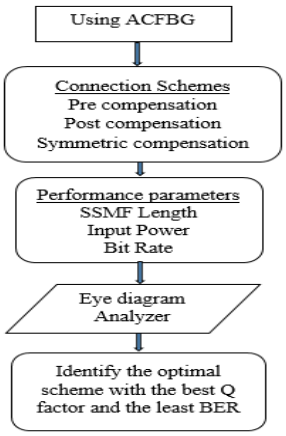

Fig. 4. Flowchart of the comparative study.

TABLE I COMPONENTS AND THEIR SIMULATION PARAMETERS

Components	Parameters
PRBS generator	Data rate: 10 Gbps
RZ pulse generator	Duty cycle: 0.5
Continuous Wave Laser	Input power: 3 dBm Linewidth: 0.01 MHz Central frequency: 193.4 THz
Mach–Zehnder Modulator	Extinction ratio: 30 dB
Standard Single-mode fiber (SSMF-28)	Length: 10 km to 80 km Attenuation loss: 0.18 dB/km Dispersion: 16.5 ps/nm/km Dispersion slope: 0.05 ps/nm^2/km Core effective area: 76.5 μm^2
FBG	Grating Length: 7 mm Effective index: 1.45 Apodization function: Gaussian Gauss parameter: 0.5 Chirp Function: Linear Linear Parameter: 0.0001 μm
EDFA optical amplifier	Gain: 10 dB Noise figure: 4 dB
PIN photodetector	Responsivity: 1 A/W Dark current: 10 nA
LPG filter	cutoff frequency: 0.75 × Bit rate

The study compares three compensation methods:

A. Case One: Pre-Compensation Scheme

In the pre-compensation setup, illustrated in Fig. 5, the ACFBG is positioned at the transmitter side, between the MZM and the SSMF. This arrangement enables early compensation for chromatic dispersion by introducing negative dispersion before the optical signal propagates through the fiber. The ACFBG's linear chirp profile and Gaussian apodization help match the anticipated dispersion profile while suppressing sidelobes and enhancing signal integrity.

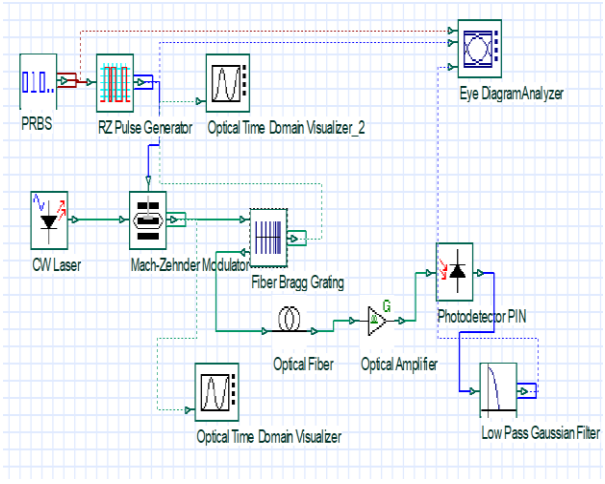

Fig. 5. Pre-compensation model for chromatic dispersion mitigation.

B. Case Two: Post-Compensation Scheme

In the post-compensation setup presented in Fig. 6, the ACFBG is placed at the receiver side, between the SSMF and the EDFA optical amplifier. As the optical signal traverses the SSMF, it accumulates positive chromatic dispersion due to the fiber's physical characteristics. The ACFBG introduces negative dispersion that compensates for this accumulated distortion. The placement of the EDFA after the ACFBG helps amplify the restored signal to meet the detection threshold of the PIN photodetector, ensuring accurate recovery of the transmitted information.

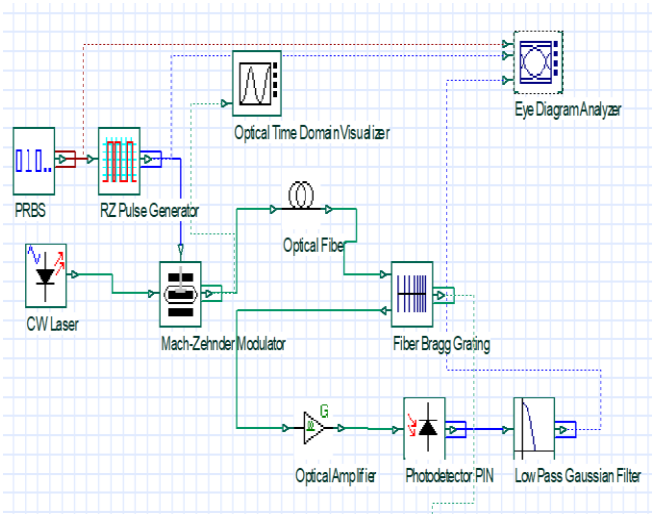

Fig. 6. Post-compensation model for chromatic dispersion mitigation.

C. Case Three: Symmetrical Compensation Scheme

The symmetrical compensation configuration, depicted in Fig. 7, comprises two ACFBGs, one located at the transmitter and the other at the receiver. The first ACFBG, situated between the MZM and the EDFA optical amplifier, provides pre-compensation, mitigating dispersion before fiber transmission. The second ACFBG, placed between the SSMF and the receiver-side EDFA optical amplifier, applies post-compensation to eliminate residual dispersion. This dual-stage configuration balances dispersion across the link and helps preserve pulse shape, thereby minimizing inter-symbol interference and improving overall system robustness. EDFAs placed before and after the SSMF maintain optimal power levels throughout the transmission path.

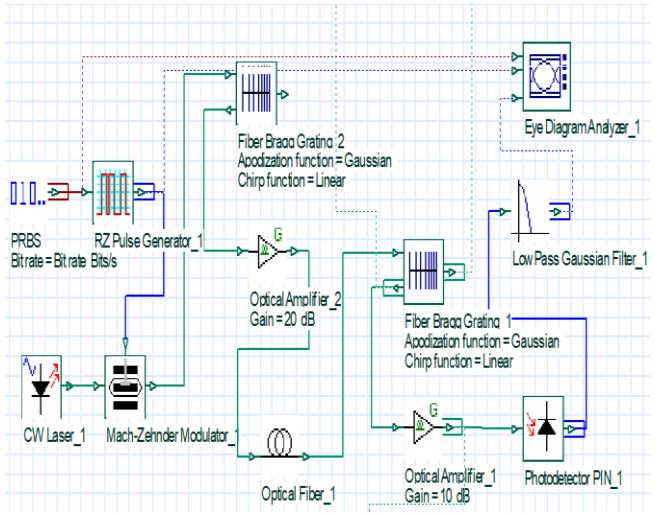

Fig. 7. Symmetrical compensation model for chromatic dispersion mitigation.

V. RESULTS

This section presents simulation results obtained using OptiSystem 7.0 to evaluate the performance of pre-, post-, and symmetrical dispersion compensation schemes. The system was tested under varying SSMF lengths, input power levels, and bit rates. Key performance metrics include Q-factor, BER, and eye height.

A. Performance with Varying SSMF Lengths

Simulations were conducted by varying the SSMF length from 10 km to 80 km, with fixed parameters: bit rate = 10 Gbps, input power = 3 dBm, and FBG length = 7 mm. Table II summarizes the results. Fig. 8 shows the eye diagram for the pre-compensation scheme at 80 km. It reveals a nearly closed eye pattern with Q-factor = 1.71181, BER = 0.0430757, and eye height = -3.43222×10^{-5}, indicating severe dispersion-induced degradation. Fig. 9 displays the eye diagram for the post-compensation scheme at 80 km. It exhibits similar degradation with Q-factor = 1.74339, BER = 0.0403394, and eye height = -3.33765×10^{-5}. Fig.10 illustrates the symmetrical compensation scheme at 80 km. The eye remains open with Q-factor = 12.3938, BER = 1.12336×10^{-35}, and eye height = 0.00215177, indicating robust signal quality. Fig. 11 presents the Q-factor performance over increasing SSMF lengths. While pre- and post-compensation schemes decline steadily beyond 50 km, symmetrical compensation maintains significantly higher Q-factors. Fig. 12 shows the corresponding BER trend. BER for pre- and post-compensation increases exponentially with distance, while symmetrical compensation sustains extremely low BER values up to 80 km.

TABLE II COMPARISON OF DISPERSION COMPENSATION OVER VARYING FIBER LENGTHS

SSMF Length	Q Factor	BER	Eye Height
Pre-compensation			
10km	204.277	0	0.00322713
20km	144.407	0	0.00196823
30km	94.3325	0	0.00110288
40km	27.6656	8.32188e-169	0.000541479
50km	10.7053	4.50313e-027	0.000217269
60km	6.55781	2.23474e-011	8.90316e-005
70km	3.199	0.00064678	5.44249e-006
80km	1.71181	0.0430757	-3.43222e-005
Post-compensation			
10km	225.662	0	0.00322955
20km	146.268	0	0.001974
30km	88.2633	0	0.00110687
40km	27.3885	1.71148e-165	0.000545474
50km	10. 9445	3.30286e-028	0.000221097
60km	6.76954	5.22884e-012	9.26084e-005
70km	3.22965	0. 000582328	6.31461e-006
80km	1.74339	0.0403394	-3.33765e-005
Symmetrical compensation			
10km	257.323	0	0.0986005
20km	251.65	0	0.0659836
30km	185.795	0	0.0439226
40km	123.736	0	0.0265569
50km	57.0918	0	0.0155047
60km	39.5139	0	0.00877851
70km	21.0042	2.48577e-098	0.00426993
80km	12.3938	1.12336e-035	0. 00215177

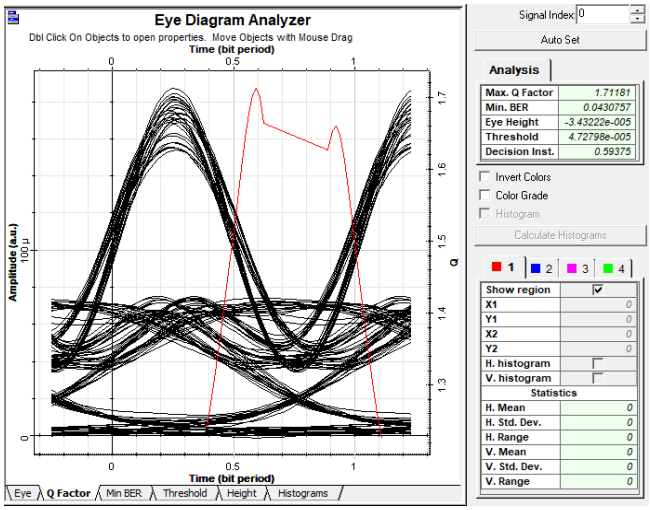

Fig. 8. Eye diagram for pre-compensation at 80 km SSMF: Q-factor = 1.71181, BER = 0.0430757, eye height = -3.43222×10^{-5}.

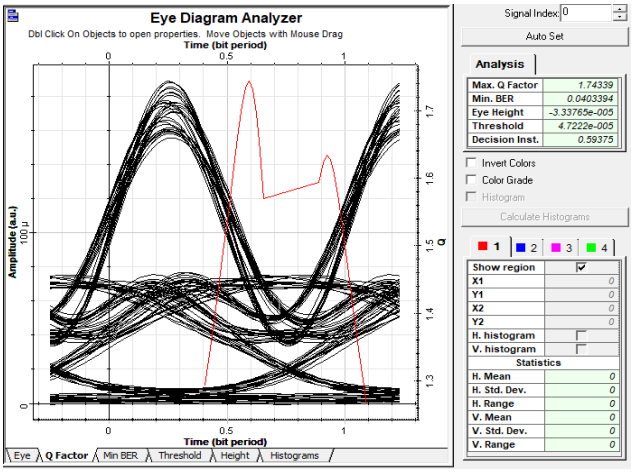

Fig. 9. Eye diagram for post-compensation at 80 km SSMF: Q-factor = 1.74339, BER = 0.0403394, eye height = 3.33765×10^{-5}.

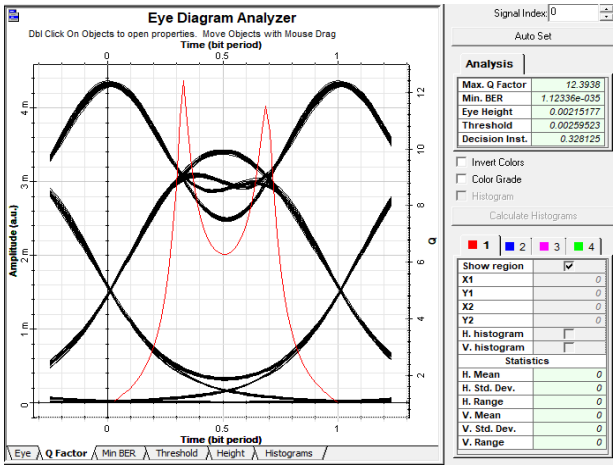

Fig. 10. Eye pattern of the symmetrical compensation scheme at 80 km SSMF length, having a Q-factor of 12.3938, BER of 1.12336×10^{-35}, and an eye height of 0.0021517.

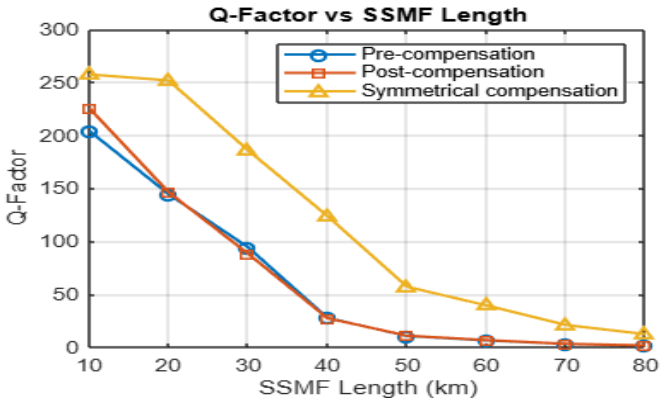

Fig. 11. Q-factor comparison of pre-, post-, and symmetrical compensation schemes over SSMF lengths from 10 km to 80 km.

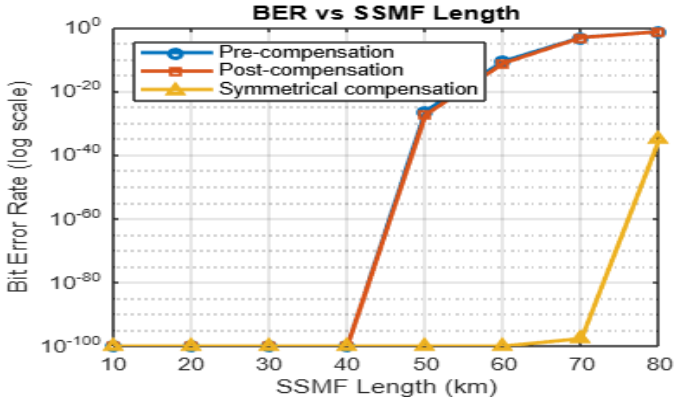

Fig. 12. BER comparison of pre-, post-, and symmetrical compensation schemes over SSMF lengths from 10 km to 80 km.

B. *Effect of Input Power*

To evaluate power efficiency, input power levels were varied between 0 dBm and 10 dBm, with fixed parameters: 60 km SSMF, 7 mm FBG length, and 10 Gbps bit rate. Results are presented in Table III. Fig. 13 shows the eye diagram for pre-compensation at 3 dBm, where the Q-factor is 6.5578, BER = 2.23474×10^{-11}, and eye height = 8.90316×10^{-5}. Fig. 14 illustrates the post-compensation performance at 3 dBm. It yields a Q-factor of 6.76954, BER = 5.22884×10^{-12}, and eye height = 9.26084×10^{-5}. Fig. 15 depicts the symmetrical compensation scheme at the same power level, with superior performance: Q-factor = 39.5139, BER = 0, and eye height = 0.00877851. Fig. 16 plots the Q-factor versus input power. All schemes improve as power increases, but symmetrical compensation peaks at 3 dBm before slightly declining. Fig. 17 presents the BER variation across the power range. Symmetrical compensation maintains ultra-low BER at lower powers, while other schemes improve gradually.

C. *Impact of Bit Rate*

To assess the performance at higher data rates, Bit rate was varied from 5 Gbps to 20 Gbps, keeping SSMF = 60 km, input power = 3 dBm, and FBG length = 7 mm. The results are shown in Table IV. Fig. 18 shows the pre-compensation scheme at 15 Gbps. The signal completely fails with Q = 0, BER = 1, and a closed eye. Fig. 19 illustrates similar failure for the post-compensation scheme at 15 Gbps, also showing Q = 0 and BER = 1. Fig. 20 shows that the symmetrical compensation scheme still maintains acceptable signal integrity at 15 Gbps, with Q-factor = 3.13256, BER = 0.000848, and eye height = 0.0001717. Fig. 21 displays the Q-factor drop with increasing bit rate. Symmetrical compensation performs best, sustaining up to 15 Gbps. Fig. 22 confirms this trend in BER values, where pre- and post-compensation fail beyond 10 Gbps, while symmetrical compensation remains viable until 15 Gbps.

TABLE III INPUT POWER IMPACT ON FBG-BASED DISPERSION COMPENSATION SCHEMES

Pre compensation			
Input power	**Q Factor**	**BER**	**Eye height**
1 dBm	6.29833	1.26638e-010	5.41366e-005
3 dBm	6.55781	2.23474e-011	8.90316e-005
5 dBm	6.75313	5.8059e- 012	0.000144925
7 dbm	6.91703	1.83027e-012	0.000235027
9 dbm	7.07983	5.71629e-013	0.000381608
10 dbm	7.17114	2.95391e-013	0.000487903
Post compensation			
1 dBm	6.48034	3.82134e-011	5.6213e-005
3 dBm	6.76954	5.22884e-012	9.26084e-005
5 dBm	7.00624	9.77794e-013	0.000151683
7 dBm	7.2343	1.8825e-013	0.000248944
9 dBm	7.51008	2.446e-014	0.000417761
10dBm	7.69198	6.13173e-015	0.000545276
Symmetrical compensation			
1 dBm	18.6572	5.50605e-078	0.00412606
3 dBm	39.5139	0	0.00877851
5 dBm	15.7013	7.40624e-056	0.0111316
7 dBm	4.05863	2.4589e-005	0.00262278
9 dBm	4.14571	1.3133e-005	0.00369366
10 dBm	4.03821	2.4014e-005	0.00541803

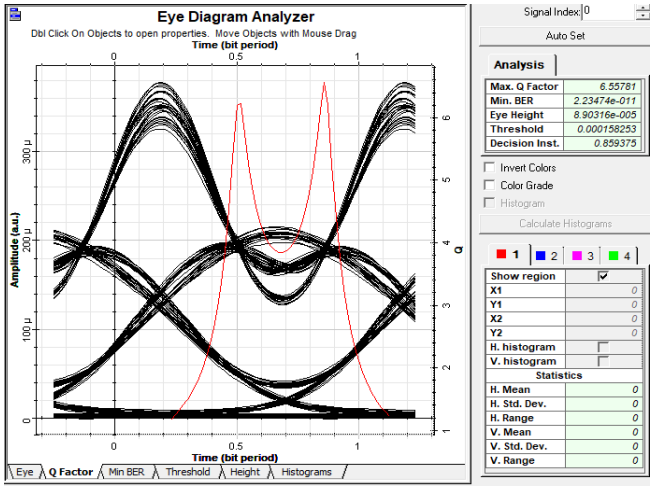

Fig. 13. Eye diagram for pre-compensation at 3 dBm input power with Q-factor 6.56, BER 2.23×10^{-11}, and eye height 8.9×10^{-5}.

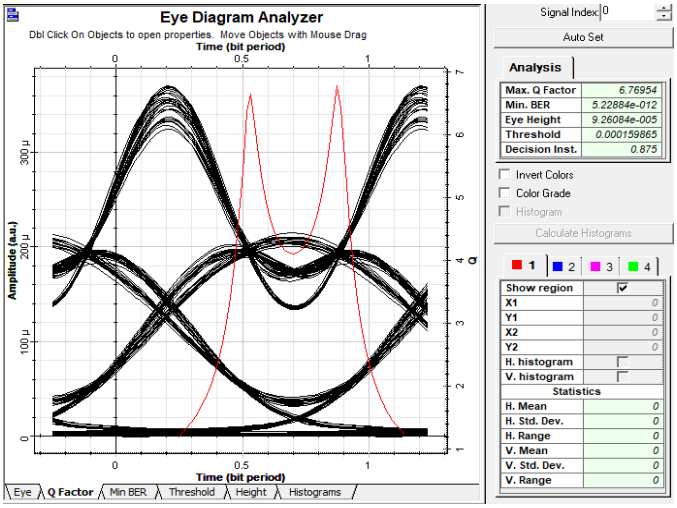

Fig. 14. Eye diagram for post-compensation at 3 dBm input power with Q-factor 6.77, BER 5.23×10^{-12}, and eye height 9.26×10^{-5}.

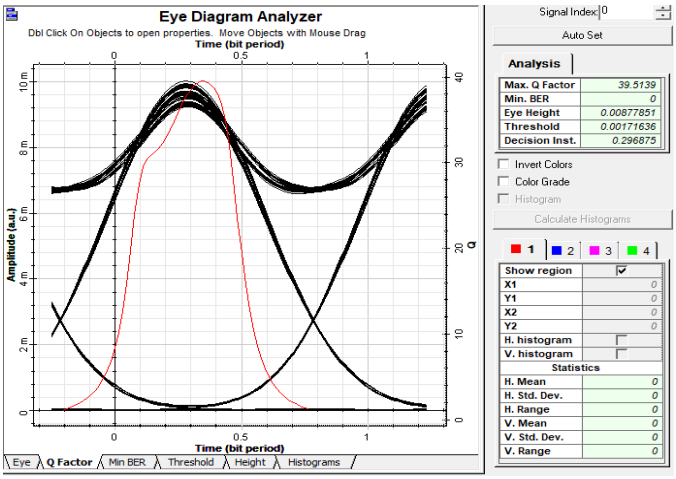

Fig. 15. Eye diagram for symmetrical compensation at 3 dBm input power with Q-factor 39.51, BER 0, and eye height of 0.00877851.

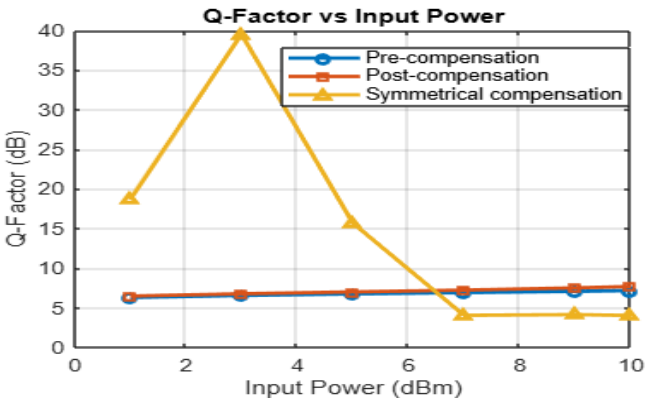

Fig. 16. Q-factor variation with input power across different dispersion compensation schemes.

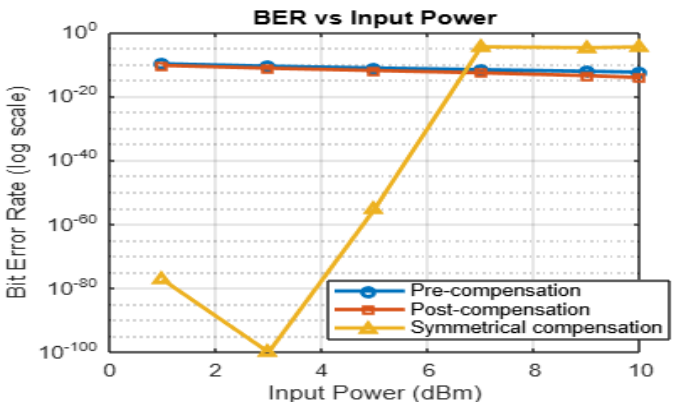

Fig. 17. BER variation with input power for different dispersion compensation configurations.

TABLE IV COMPENSATION SCHEME PERFORMANCE ACROSS VARIOUS BIT RATES

Pre-compensation			
Bit rate	**Q Factor**	**BER**	**Eye Height**
5 Gbps	77.3924	0	0.000572817
10 Gbps	6.55781	2.23474e-011	8.90316e-005
15 Gbps	0	1	0
20 Gbps	0	1	0
Post-compensation			
5 Gbps	87.9373	0	0.000580293
10 Gbps	6.76954	5.22884e-012	9.26084e-005
15 Gbps	0	1	0
20 Gbps	0	1	0
Symmetrical compensation			
5 Gbps	376.066	0	0.0275402
10 Gbps	39.5139	0	0.00877851
15 Gbps	3.13256	0.000848086	0.000171737
20 Gbps	0	1	0

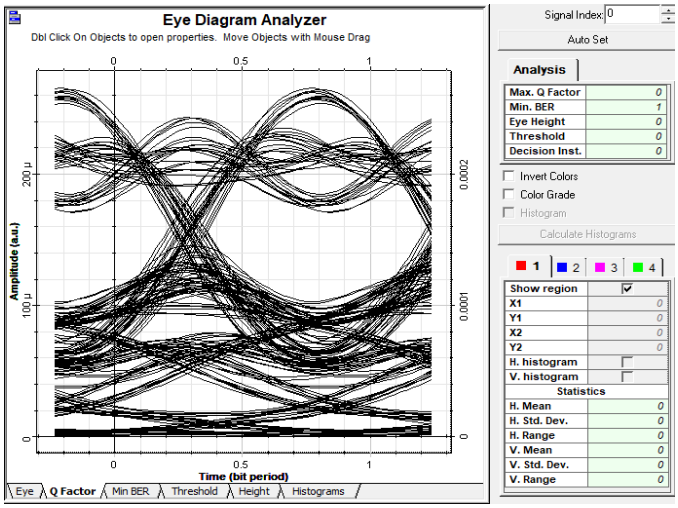

Fig. 18. Eye diagram for pre-compensation at 15 Gbps showing Q-factor 0, BER 1, and eye height 0.

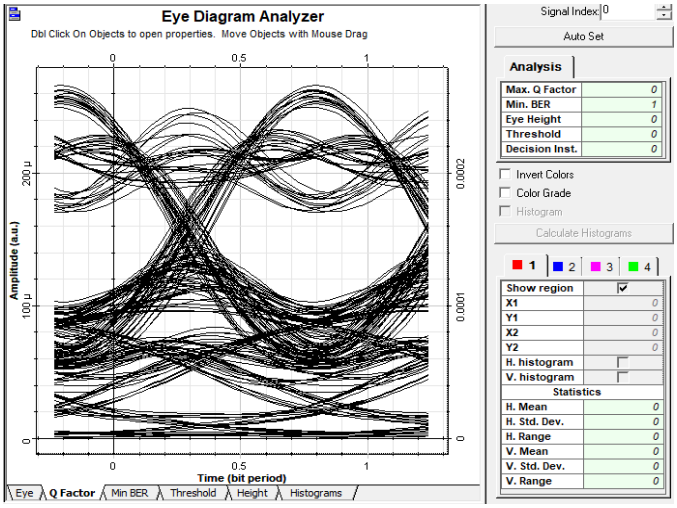

Fig. 19. Post-compensation scheme at 15 Gbps bit rate, showing a Q-factor of 0, BER of 1, and eye height of 0.

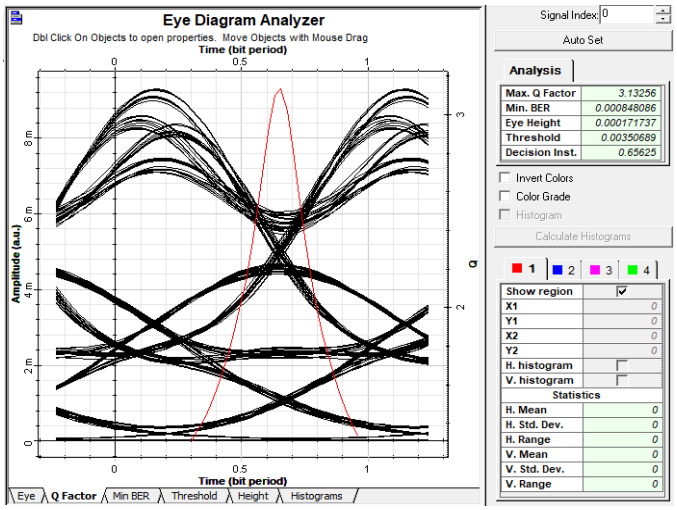

Fig. 20. Eye diagram for symmetrical compensation at 15 Gbps with Q-factor 3.13, BER of 0.000848086, and eye height of 0.000171737.

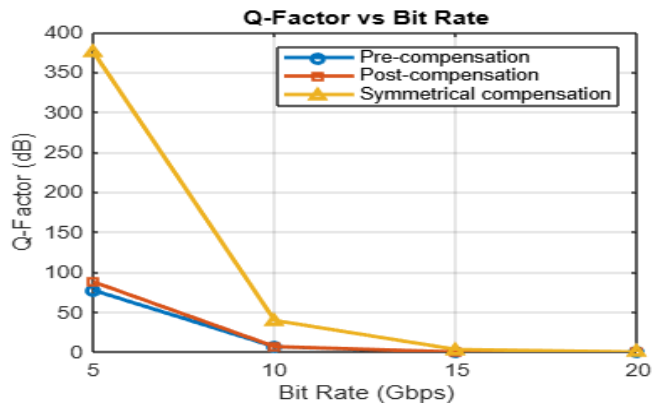

Fig. 21. Q-factor variation versus bit rate for pre-, post-, and symmetrical dispersion compensation schemes.

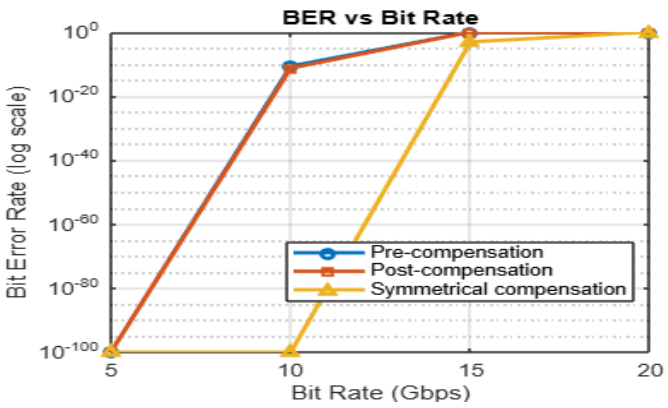

Fig. 22. Comparison of BER at various bit rates for pre-, post-, and symmetrical compensation.

The dataset used in this study was entirely generated using OptiSystem 7.0 and includes simulated performance metrics (Q-factor, BER, and eye height) across varying SSMF lengths (10–80 km), input powers (0–10 dBm), and data rates (5–20 Gbps). It is simulation-based, with no physical measurements or external inputs, and its accuracy depends on the fidelity of the OptiSystem simulation models.

VI. Discussion

This section interprets the results presented in Section V, emphasizing the performance trade-offs and advantages of each compensation approach.

A. Interpretation of SSMF Length Results

Symmetrical compensation consistently delivers superior performance compared to the other two compensation schemes. While the pre- and post-compensation approaches exhibit significant performance degradation beyond 50 km dropping to a Q-factor of approximately 1.72 and a BER around 0.04 at 80 km. Symmetrical compensation maintains high signal quality, achieving a Q-factor of 12.39, an ultra-low BER of 1.12×10^{-35}, and an improved eye height. These results highlight symmetrical compensation as the most reliable and efficient approach for long-haul, high-speed optical communication systems.

B. Power Efficiency Evaluation

The pre- and post-compensation schemes show consistent improvement in performance as the input power increases. Both demonstrate a gradual rise in Q-factor and a corresponding reduction in BER as power increases from 1 dBm to 10 dBm. At 9–10 dBm, both schemes reach a Q-factor of approximately 7 and achieve BER values on the order of 10^{-13}, indicating reliable signal quality at higher power levels. Between the two, post-compensation performs slightly better, offering higher Q-factors and lower BERs across the entire power range. In contrast, symmetrical compensation stands out by delivering excellent performance at significantly lower power. It achieves a remarkably high Q-factor of 39.51 and zero BER at just 3 dBm input power, along with the largest eye opening (eye height = 0.00878). Although its performance varies at higher power levels, the ability to attain optimal results at minimal input power underscores symmetrical compensation as the most

power-efficient solution, especially suitable for systems where energy efficiency is critical.

C. Bit Rate Performance

Pre- and post-compensation schemes fail to support bit rates beyond 10 Gbps, with Q-factors dropping to zero and BER reaching 1. In contrast, symmetrical compensation maintains acceptable performance up to 15 Gbps, attained a Q-factor of 3.13 and a BER of 8.48×10^{-4}. Although slightly degraded, this outcome confirms the scalability of symmetrical compensation for higher data rates. These results are consistent with the observed Q-factor and BER trends and are further supported by corresponding eye diagram evaluations.

D. Comparison of Proposed and Existing Methods

To validate the efficiency of the proposed dispersion compensation scheme, its performance is compared against several established methods from the literature. Table V summarizes key metrics such as Q-factor and BER across different compensation strategies, fiber lengths, and grating parameters. While most prior studies focus on post-compensation and evaluate transmission distances up to 70 km, this work demonstrates that the symmetrical compensation scheme using Gaussian-ACFBGs not only supports long-haul transmission over 80 km but also achieves a notably higher Q-factor (12.39) and an ultra-low BER (1.12×10^{-35}). These results outperform existing designs without relying on cascading or hybrid filtering techniques. The results clearly demonstrate the superior efficiency of the proposed scheme in long-haul optical transmission scenarios, establishing it as a competitive alternative to traditional post-compensation techniques.

TABLE V COMPARISON OF PROPOSED SCHEME WITH PRIOR WORKS

Prior Research	Compensation schemes with best results	SSMF Length(km)	Grating length (mm)	Q factor	BER
[18]	Post-compensation	50	-	45.78	0
[19]	Post-compensation	40	6	29.55	9.3407×10^{-182}
[20]	Post-compensation	70	2	8.58	4.77×10^{-18}
[21]	Post-compensation	70	2	9.2	3.25×10^{-20}
[22]	Post-compensation	80	2,3	6.848	3.73×10^{-12}
[23]	Post-compensation	30	-	23.647	Not given
[24]	Post-compensation	70	5	7.22	2.59×10^{-13}
Proposed Work	Symmetrical-compensation	80	7	12.3938	1.12336×10^{-35}

E. Physical Mechanism behind Performance Improvement

The symmetrical compensation scheme using Gaussian ACFBGs performs best because it balances dispersion correction by placing compensating gratings at both ends of the fiber. The linear chirp in the grating reflects different wavelengths at specific points, accurately compensating for dispersion. Gaussian apodization reduces unwanted side lobes, thereby lowering signal distortion. By dividing the compensation into two stages, this method reduces nonlinear effects, phase distortion, and jitter more effectively than pre- or post-compensation alone. As a result, it delivers cleaner signals with higher Q-factors, lower BER, and better eye diagrams, making it highly suitable for long-distance, high-capacity optical communication systems.

VII. CONCLUSION

This research investigates dispersion compensation in optical communication systems using Gaussian-apodized, linear-chirped Fiber Bragg Gratings. Three compensation schemes pre-compensation, post-compensation, and symmetrical compensation, were evaluated over an 80 km SSMF link. At this distance, pre-compensation achieved a Q-factor of 1.71181, BER of 0.0430757, and an eye height of -3.43222×10^{-5}, while post-compensation slightly improved performance with a Q-factor of 1.74339, BER of 0.0403394, and eye height of -3.33765×10^{-5}. In contrast, symmetrical compensation significantly outperformed both, achieving a Q-factor of 12.3938, an ultra-low BER of 1.12336×10^{-35}, and an eye height of 0.00215177. These results demonstrate that symmetrical compensation offers the most effective solution for long-haul, high-speed optical transmission, meeting the stringent requirements of 5G networks, especially in fronthaul and backhaul scenarios. This supports key 5G applications such as ultra-reliable low-latency communication (URLLC), enhanced mobile broadband (eMBB), and massive machine-type communication (mMTC). Furthermore, optimization of input power and bit rate enhances energy efficiency and scalability, making the approach suitable for smart cities, industrial automation, and remote healthcare systems. The proposed technique provides several advantages: it passively compensates dispersion without the need for active electronic components, thereby reducing power consumption; Gaussian apodization effectively suppresses sidelobes to improve signal quality; the chirped grating profile allows for tailored dispersion management over long distances; and the configuration is both scalable and compatible with existing fiber infrastructures. These attributes establish symmetrical ACFBGs as a highly efficient, high-performance, and future-proof solution for optical networks.

FUTURE WORK

Future work may explore system performance under higher-order modulation formats, assess the impact of temperature variations and polarization sensitivity, and investigate hybrid approaches that integrate FBGs with adaptive, machine learning–based equalizers. Additionally, the influence of channel spacing in dense WDM environments and the potential for real-time tunability using dynamic gratings could be examined to enhance system adaptability in evolving optical networks. Overall, this study demonstrates that symmetrical FBG-based dispersion compensation is a robust, scalable, and forward-looking solution for next-generation 5G optical infrastructure.

ACKNOWLEDGMENT

The authors express their sincere gratitude to Cambridge Institute of Technology, Bengaluru, and the Visvesvaraya

Technological University, Belagavi, for their valuable support and scholarly guidance during the course of this research.

REFERENCES

[1] E. Nsengiyumva, G. Mwangi, and Kamucha, "A comparative study of chromatic dispersion compensation in 10Gbps SMF and 40Gbps OTDM systems using a cascaded Gaussian linear apodized chirped fibre Bragg grating design," Heliyon, vol. 8, no. 4, Article. 9308, 2022.

[2] A .B. Dar and R. K. Jha, "Chromatic dispersion compensation techniques and characterization of fiber Bragg grating for dispersion compensation," Opt Quant Electron, vol. 49, no. 3, p. 108, 2017.

[3] A. Mahmoud, Y.A El-Salam, M. Ahmed, and T. Mohamed, "Effect of fiber properties and dispersion management on distortions associated with two subcarriers modulation of laser diode in radio over fiber systems," The European Physical Journal D, vol. 76, no. 11, p. 229, 2022.

[4] R. K. Gupta and M. L. Meena, "Investigation of long-haul optical transmission systems: diverse chirped FBGs with DCF for 300 km length of SMF,"International Journal of Advanced Technology and Engineering Exploration, vol. 9, no. 97, pp. 1757–1766, 2022.

[5] Z. Lv, J. Du, and Z. He, "On-chip multichannel dispersion compensation and wavelength division MUX/DeMUX using chirped-multimode-grating-assisted counter-directional coupler," Photonics, vol. 11, no. 2, p. 110, Jan. 2024.

[6] I. Nsengiyumva, E. Mwangi, and G. Kamucha, "Performance analysis of a linear Gaussian- and tanh-apodized FBG and dispersion compensating fiber design for chromatic dispersion compensation in long-haul optical communication networks," International Journal of Optics, vol. 2022, Art. no. 5734420, pp. 1–14, Sep. 2022.

[7] F. M. Mustafa, A. F. Sayed, and M. H. Aly, "A reduced power budget and enhanced performance in a WDM system: a new fbg apodization function," Optical and Quantum Electronics, vol. 54, no. 8, p. 471, 2022.

[8] F. M. Mustafa, S. A. Zaky, A. A. M. Khalaf, and M. H. Aly, "Chromatic dispersion compensation by cascaded FBG with duobinary modulation scheme," Optical and Quantum Electronics, vol. 54, no. 12, p. 819, 2022.

[9] N. A. Mohammed and N. M. Okasha, "Single- and dual-band dispersion compensation unit using apodized chirped fiber Bragg grating," J Comput Electron, vol. 17, no. 1, pp. 349–360, 2018.

[10] S. Ranathive, K. V Kumar, A. N. Z Rashed, M. S. F. Tabbour and T.V.P. Sundararajan,"Performance Signature of Optical Fiber Communications Dispersion Compensation Techniques for the Control of Dispersion Management," Journal of Optical Communications, vol. 43, no. 4, pp. 611–623, 2019.

[11] Jyotsanaa, R. Kaura and R. Singh, "Performance comparison of pre-, post- and symmetrical dispersion compensation techniques using DCF on 40Gbps OTDM system for different fibre standards," Optik, vol. 125, no. 9, pp. 2134–2136, 2014.

[12] M. Sharma and D. Kumar, "Dispersion Compensation for 40 Gbps Optical Waveguide System by Using FBG," in Proc of "3rd International Conference and Workshops on Recent Advances and Innovations in Engineering (ICRAIE), 2018, pp. 1–3.

[13] A. F. Sayed, T. M. Barakat, and I. A. Ali, "A Novel Dispersion Compensation Model using an Efficient CFBG Reflectors for WDM Optical Networks," International Journal Of Microwave and Optical Technology, vol. 12, no. 3, pp. 230–238, 2017.

[14] R. Udayakumar, V. Khanaa, and T. Saravanan,"Chromatic Dispersion Compensation in Optical Fiber Communication System and its Simulation," Indian Journal of Science and Technology, vol. 6, no. 6S, pp. 4762–4766, 2013.

[15] M. L. Meena and R. K. Gupta, "Design and comparative performance evaluation of chirped FBG dispersion compensation with DCF technique for DWDM optical trans- mission systems," International Journal for Light and Electron Optics, vol. 188, no. 1, pp. 212–224, 2019.

[16] D. Irawan, Azhar, and K. Ramadhan, "High-Performance Compensation Dispersion with Apodization Chirped Fiber Bragg Grating for Fiber Communication System," Jurnal Penelitian Pendidikan IPA, vol. 8, no. 2, pp. 992– 999, 2022.

[17] B. Yousif, A. Sh. Samrah, and R. Waheed, "High Quality Factor and Dispersion Compensation Based on Fiber Bragg Grating in Dense Wavelength Division Multiplexing," Optical Memory and Neural Networks, vol. 29, no. 3, pp. 228–243, 2020.

[18] M. A. A. Almuhsan, "Performance Evaluation of Various Dispersion Compensation Techniques," Journal of Optics, vol. 53, no. 3, 2024.

[19] F. Keti, "A New Proposed Model for Dispersion Compensation via Linear Chirped Fiber Bragg Grating," Traitement du Signal, vol. 41, no. 1, pp. 451–457, 2024.

[20] F. M. Mustafa, A. Mohamed, A. A. M. Khalaf, A. F. Sayed, and M. H. Aly, "Dispersion compensation using cascaded apodized CFBGs under MTDM transmission technique: Enhanced system performance," Optical and Quantum Electronics, vol. 55, no. 1, p. 32, 2022.

[21] F. M. Mustafa, H. A. Kholidy, A. F. Sayed, and M. H. Aly, "Enhanced dispersion reduction using apodized uniform fiber Bragg grating for optical MTDM transmission systems," Optical and Quantum Electronics, vol. 55, no. 1, p. 55, 2022.

[22] T. K. Panda, A. B. M K. Behera, and S. Polei, "Performance comparison of Fiber Bragg Grating for different Grating length, Apodization function and Chirp function," in Proc. of 2020 International Conference on Computer Science, Engineering and Applications (ICC- SEA), 2020, pp. 1–5.

[23] M. Chakkour, O. Aghzout, B. A. Ahmed, F. Chaoui, and M. E. Yakhloufi, "Chromatic Dispersion Compensation Effect Performance Enhancements Using FBG and EDFA-Wavelength Division Multiplexing Optical Transmission System," Hindawi International Journal of Optics, vol. 6428972, pp. 1–8, 2017.

[24] F. M. Mustafa, S. A. Zaky, A. A. M. Khalaf, and M. H. Aly, "A cascaded FBG scheme based OQPSK/DPSK modulation for chromatic dispersion compensation," Optical and Quantum Electronics, vol. 54, no. 7, p. 429, 2022.

[25] A. Onoufriou, K. Kalli, D. Pureur, and A. Mugnier, "Fibre Bragg Gratings," Springer Series in Optical Sciences, vol. 123, pp. 189–269, 2006.

[26] M. Mustafa, M. M. Abdelhalim, M. H. Aly, and T. M. Barakat, "Dispersion compensation analysis of optical fiber link using cascaded apodized FBGs hybrid with maximum time division multiplexing transmission technique," Optical and Quantum Electronics, vol. 53, no. 7, p. 358, 2021.

[27] A. F Sayed, F. M. Mustafa, A. A. M. Khalaf, and M. H. Aly, "Symmetrical and post-dispersion compensation in WDM optical communication systems," Opt Quant Electron, vol. 53, no.1, pp. 37–56, 2021.

[28] D. A. Egorova, A. V. Kulikov, A. N. Nikitenk, A. I. Gribaev, and S. V. Varzhel, "Investigation of bending effects in chirped FBGs array in multicore fiber," Optical and Quantum Electronics, vol. 52, no. 2, p. 130, 2020.

[29] N. A. Mohammed, M. Solaiman, and M. H. Aly, "Design and performance evaluation of a dispersion compensation unit using several chirping functions in a tanh apodized FBG and comparison with dispersion compensation fiber," Applied Optics, vol. 53, no. 29, pp. 239–247, 2014.

[30] T. F. Hussein, M. R. M. Rizk, and M. H. Aly, "A hybrid DCF/FBG scheme for dispersion compensation over a 300 km SMF," Optical and Quantum Electronics, vol. 51, no. 4, p. 103, 2019.

[31] D. Meena and M. L. Meena, "Design and Analysis of Novel Dispersion Compensating Model with Chirp Fiber Bragg Grating for Long-Haul Transmission System," Lecture Notes in Electrical Engineering Optical and Wireless Technologies, vol. 546, pp. 29–36, 2023.

[32] A. F. Sayed, F. M. Mustafa, A. A. M. Khalaf, and M. H. Aly, "An enhanced WDM optical communication system using a cascaded fiber Bragg grating," Optical and Quantum Electronics, vol. 52, no. 3, p. 181, 2020.

[33] A. F. Sayed, F. M. Mustafa, A. A.M. Khalaf and M. H. Aly, "Apodized chirped fiber Bragg grating for post-dispersion compensation in wavelength division multiplexing optical networks," International Journal of Communication System, vol. 33, no. 2, p. 4551, 2020.